Control of molecular dissociation by spatially inhomogeneous near fields

I. Yavuz,[1,*] J. Schötz,[2,3] M. F. Ciappina,[2,4] P. Rosenberger,[2,3] Z. Altun,[1] M. Lewenstein,[5,6] and M. F. Kling[2,3,*]

[1]*Physics Department, Marmara University, Ziverbey, 34722 Istanbul, Turkey*

[2]*Max-Planck-Institut für Quantenoptik, Hans-Kopfermann-Straße 1, 85748 Garching, Germany*

[3]*Department of Physics, Ludwig-Maximilians-Universität Munich, Am Coulombwall 1, 85748 Garching, Germany*

[4]*ELI Beamlines, Institute of Physics of the ASCR, Na Slovance 2, 182 21 Prague, Czech Republic*

[5]*ICFO-Institut de Ciencies Fotoniques, The Barcelona Institute of Science and Technology, 08860 Castelldefels (Barcelona), Spain*

[6]*ICREA, Pg. Lluís Companys 23, 08010 Barcelona, Spain*

(Received 29 June 2018; published 8 October 2018)

Tailored intense laser fields can be used to steer electron and nuclear dynamics in molecules and control chemical reactions. Here we demonstrate that inhomogeneous nanoscopic near fields provide an additional mechanism for controlling light-induced chemical reactions. This is investigated by quantum-dynamical calculations on dissociation of H_2^+ in few-cycle near fields with a controlled carrier-envelope phase. Directional dissociation asymmetry analysis reveals that the spatial asymmetry of the field is critical in controlling and in modifying field-induced dissociation pathways such as zero-photon dissociation, bond softening, and above-threshold dissociation. The degree of impact strongly depends on the maximum length scale of coherent control in a dissociation channel. The results pave the way towards coherent control of molecular reactions in a wide range of molecules in inhomogeneous near fields.

DOI: 10.1103/PhysRevA.98.043413

I. INTRODUCTION

Experimental and theoretical studies of the interaction of intense light pulses with molecular hydrogen have been prototypical and illuminated fundamental processes such as strong-field ionization [1], field-dressed states resulting in bond softening and bond hardening [2–6], ultrafast (coupled) electronic-nuclear wave-packet motion [7–13], laser-induced alignment [14,15], high-order harmonic generation [16], and the control of chemical reactions with the waveform of the electric field [17–34]. The vast majority of the theoretical research in this area has only considered spatially homogeneous laser fields, i.e., where electric fields $E(\mathbf{r}, t) = E(t)$ are only functions of time. This is a legitimate hypothesis, considering that the laser field changes at most on the scale of the wavelength (typically 800–3000 nm), while a laser focus spans several tens to a few hundred micrometers [35]. Additionally, the electron dynamics is typically constrained to a few tens of nanometers, even for the larger-wavelength cases. Thus, the electron is unable to experience any spatial variation of the laser field. In contrast, near fields around nanostructures are spatially dependent on a nanometer scale. The local fields can reach much larger amplitudes as compared to the incident fields, a phenomenon known as field enhancement. Experimental and theoretical studies have explored laser-matter phenomena driven by enhanced near fields [36,37], including above-threshold and strong-field ionization [38–51], electron acceleration [52,53] and recollision dynamics [54–61], and high-harmonic generation in solids [62,63]. The waveforms of nanoscale near fields have been resolved with attosecond and femtosecond spectroscopy [45,64,65].

In a broader context, near fields open a wide range of possibilities to enhance and/or shape spectral and spatial properties of an incoming field [66]. In strong few-cycle fields, control of the carrier-envelope phase (CEP) ϕ permits control over the electric-field waveform [35] and in turn electron and nuclear dynamics in molecules [29]. Here near fields constitute a possibility to enable and modify the strong-field control, where the scale of the field changes is of comparable dimension to the size of the electronic excursion. Very recently, Kazuma *et al.* demonstrated the role of near fields for molecular dissociation on nanoscale structures [67]. One of the consequences of the field inhomogeneity is inversion symmetry breaking (i.e., $\phi \not\to \phi + \pi$) of the laser field, which enables additional opportunities for coherent control. Despite their clear potential and an ample range of studies of strong-field processes in atoms (for a review see [37]), studies of molecules are scarce. Recently, the manipulation of electron localization in the field enhanced dissociation of H_2^+ was theoretically explored [68]. In this study, going beyond pure ionization phenomena, we study the influence of spatially inhomogeneous near fields on a chemical reaction, the prototypical field-induced dissociation of H_2^+. The results are compared to those obtained for conventional (spatially homogeneous) fields.

II. MODEL

We solve the time-dependent Schrödinger equation (TDSE) for H_2^+ in a linearly polarized laser field near a nanotip [69]. The geometry of the nanostructure and the position of the molecule relative to the nanostructure justify an approximation for the near field as [65,70,71]

$$E(z, t) = E(t) \exp(-z/d), \tag{1}$$

*Corresponding authors: ilhan.yavuz@marmara.edu.tr, matthias.kling@lmu.de

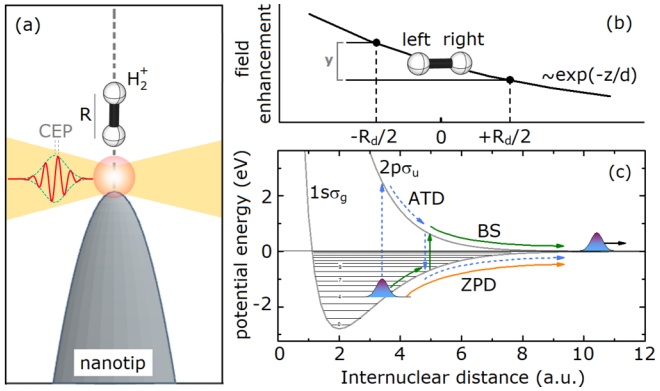

FIG. 1. (a) Schematic showing the geometry for the interaction of H_2^+ with an enhanced near field at a nanotip. The incident laser field is a few-cycle pulse with a controlled carrier-envelope phase. (b) Spatial variation of field enhancement calculation of the field asymmetry parameter y. (c) Diabatic potential energy curves and dissociation channels for H_2^+.

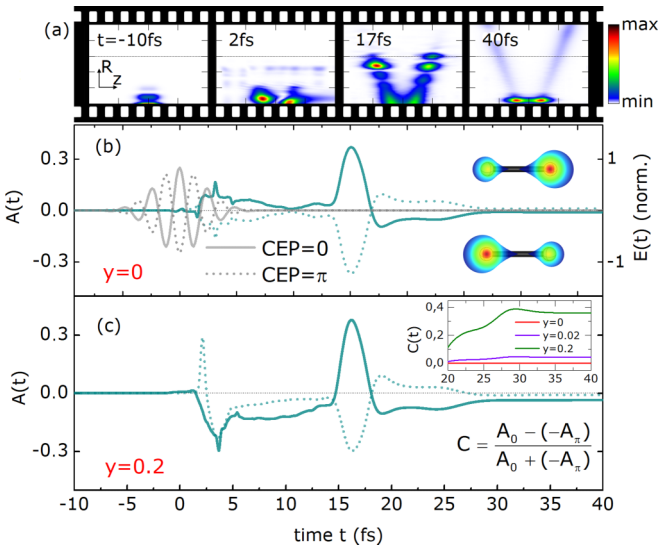

FIG. 2. (a) Instantaneous wave-packet distributions at different times. The range of the horizontal axis z is from -10.0 to $+10.0$ a.u. and the range of the vertical axis R is from 4.0 to 15.0 a.u. Horizontally dashed lines at $R_d = 10$ a.u. indicate the position of the detector (see the text). (b) Gray lines and the right axis show temporal profiles of the field $E(t)$ for $y = 0$. Blue (dark gray) lines and the left axis show variation of the dissociation asymmetry $A(t)$ for $y = 0$. (c) Same as in (b) but for $y = 0.2$. The inset shows the time dependence of the asymmetry contrast $C(t)$, as defined in the legend, near the asymptotic limit.

where d is the decay length and $d \to \infty$ implies a conventional homogeneous field (see Fig. 1). The decay length is on the order of the radius of curvature of the nanostructure and can be as small as a few nanometers. The time-dependent part of the near field is taken as $E(t) = E_0 f(t) \cos(\omega_0 t + \phi)$. Here $f(t)$, ω_0, and ϕ are the pulse envelope, laser frequency, and carrier-envelope phase (CEP), respectively, and E_0 is the field amplitude of the near field at the position of the molecule and can be enhanced by a factor of 10 compared to the incident field, depending on the nanotip's geometry [71,72]. Here we take the polarization of the laser field and molecular axis of H_2^+ to be aligned along the apex of the nanotip, as shown in Fig. 1(a), since this configuration is maximal in terms of dissociation efficiency [8]. In order to exclusively investigate the effect of the inhomogeneity of the field, we do not consider the surface of the nanostructure. The laser wavelength is $\lambda = 800$ nm and $f(t)$ is a Gaussian-shaped pulse with two-cycles (5.4-fs FWHM of the field envelope). The field intensity of the near field at the position of the molecule is chosen as $I = 240$ TW/cm^2. In order to quantify the effect of the spatial asymmetry of the field on the dissociation dynamics, we introduce an inhomogeneity parameter, the field asymmetry $y = [E(z = -R_d/2) - E(z = R_d/2)]/E_0$ [see Fig. 1(b)]. Here R_d is the distance beyond which the dissociation can be observed, which we set to 10 a.u. The y parameter is a measure of the relative difference in field strength between the left and right nuclei. Throughout the paper, we consider that the H_2^+ molecule is populated in the electronic $1s\sigma_g$ ground state and the Franck-Condon weighted superposition of the first 20 vibrational states, as obtained from the ionization of H_2, before interacting with the few-cycle laser field (i.e., at $t = -\infty$). Finally, for numerical simulations, the field-matter interaction term can be found by integrating the field $E(z,t)$ as $V(z,R,t) = \int_0^z E(z',t)dz' - \int_0^R [E(z'/2,t) - E(-z'/2,t)]dz'$, which corresponds to $V(z,t) = zE(t)$ for homogeneous fields, as expected [73]. For the case of the near field, expressed in Eq. (1), the interaction potential becomes

$$V(z,R,t) = d\{(1 - e^{-z/d}) - 4[\cosh(R/2d) - 1]\}E(t). \quad (2)$$

III. RESULTS AND DISCUSSION

To quantify the directionality during molecular dissociation, we use the asymmetry A of molecular dissociation computed from $A = (P_r - P_l)/(P_r + P_l + \varepsilon)$, where P_r (P_l) indicates dissociation probability for the positive (negative), i.e., $z \geqslant 0$ ($z \leqslant 0$), region, corresponding to electron localization on the left (right) nucleus of the dissociated molecule [19]. Additionally, we include a regularization parameter ε to avoid spurious A values when $P_r + P_l \sim 0$.

First, the time evolution of the field-driven dissociating wave packet is studied to understand the influence of y on the direction of H^+ versus H emission. We simulate the dynamics of $A(t)$ for $\phi = 0[A_0(t)]$ and $\pi[A_\pi(t)]$ [cf. Fig. 2(b)]. Dissociation probabilities are calculated by $P_{r,l}(t) = \int_0^t dt' \int j(z, R_d, t')dz$, where j is the nuclear flux density of the leaking wave packet beyond $R_d = 10$ a.u. and the limits of the second integral are set to [0, 25 a.u.] and [-25 a.u., 0] for $P_r(t)$ and $P_l(t)$, respectively. Figure 2(b) shows that for $y = 0$, the field swings the electron between the two nuclei and $A(t)$ for $\phi = 0$ begins oscillating at the rising edge of the laser field. We attribute this initial behavior to dissociation from vibrational states with high quantum number, which have a sizable probability close to R_d. By the time the field reaches beyond the maximum, higher-frequency

components (e.g., at 3ω) and irregular substructures in $A(t)$ are observed. This is due to interference of the different components of the wave packet (dissociative and bound) as well as different dissociative channels. Asymmetry decreases as the field disappears, but then a large oscillation of asymmetry emerges between ∼15 and 25 fs, due to field-free propagation of the dissociating wave packet [see snapshots in Fig. 2(a)]. Beyond this time frame, a certain fraction of the wave packet remains on the right nucleus due to trapping by the potential barrier. This asymptotic asymmetry is experimentally measurable and can be controlled by the CEP. When the CEP is changed by π, the field gets inverted and so does the resulting $A(t)$. Therefore, $A_0 = -A_\pi$ for $y = 0$. When the field asymmetry $y > 0$ is introduced, the system is not inversion symmetric anymore and the dissociation in a certain direction is expected to be favored, since the field strength experienced by each nucleus differs. Indeed, we find that the inversion symmetry of $A(t)$ between $\phi = 0$ and π is broken, as can be seen in Fig. 2(c). After the peak of the field, both $A_0(t)$ and $A_\pi(t)$ are instantly enhanced up to $|0.3|$ within $t \simeq$ 0–5 fs compared to $y = 0$. However, in the asymptotic limit, the A parameters for both $\phi = 0$ and $\phi = \pi$ are negative. This means that the electrons are more likely localized on the right nucleus. In order to better measure the influence of the field asymmetry on the breaking of the inversion symmetry, we introduce the contrast between $A_0(t)$ and $A_\pi(t)$, defined as $C = [A_0 - (-A_\pi)]/[A_0 + (-A_\pi)]$. As shown in the inset of Fig. 2(c), $C(t \to \infty)$ is zero for $y = 0$ but increases to 0.04 for $y = 0.02$ and 0.36 for $y = 0.2$. Hence, the contrast parameter increases with field asymmetry.

In order to determine the physical mechanism responsible for the field asymmetry dependence, we next investigate the energy-resolved dissociation asymmetry of H_2^+ through kinetic energy release (KER). Dissociation can primarily occur via photon transitions [8]. Based on the Floquet dressed-state theory, three major channels can lead to dissociation: (i) $1s\sigma_g \to 2p\sigma_u - 0\omega$, the zero-photon dissociation (ZPD); (ii) $1s\sigma_g \to 2p\sigma_u - \omega$, the bond softening (BS) channel [2]; and (iii) $1s\sigma_g \to 2p\sigma_u - 3\omega \to 1s\sigma_g - 2\omega$, referred to as above-threshold dissociation (ATD) [cf. Fig. 1(c)] [8,74]. In the asymptotic limit, when the dissociated wave packet is relaxed, the KER can be found from $E_{\mathrm{KER}} = n\hbar\omega - |E_{\mathrm{el},v}|$, where n is the number of absorbed photons and $E_{\mathrm{el},v}$ is the electronic energy at the vth vibrational state. Thus, due to contributions from vibrational bound levels, relatively broad spectra arise with $E_{\mathrm{KER}} \sim 0.1$–$1.5$ eV for BS and $E_{\mathrm{KER}} \sim 0.5$–$3.0$ eV for ATD (for $\lambda = 800$ nm). To obtain the energy-resolved asymmetry $A(E)$, we calculate the KER spectra $P(E)$ of the field-induced dissociation, i.e., $H_2^+ + \gamma \to H^+ + H$, employing the so-called virtual-detector method [69,75].

We now inspect the CEP dependence of the directional dissociation. Figures 3(a) and 3(b) show the KER-resolved dissociation asymmetry for two different CEP values. We see that the contrast between $\phi = 0$ and $\phi = \pi$ is zero due to inversion symmetry but it increases with the inclusion of field asymmetry, due to the fact that y causes the asymmetry to shift upward with field inhomogeneity, as shown in Fig. 3(b). Next the energy- and CEP-resolved asymmetry $A(E, \phi) = [P_l(E, \phi) - P_r(E, \phi)]/[P_l(E, \phi) + P_r(E, \phi) + \varepsilon]$ is calculated for different y and a laser intensity of $I = 240$ TW/cm^2. In general, $A(E, \phi)$ is strongly controlled by CEP in few-cycle laser fields, and studies have shown that $A(E, \phi)$ is typically periodic for $y = 0$ and follows $A(E, \phi) \sim A(E)' \cos[\phi + \phi_0(E)]$, where $A(E)'$ is the asymmetry amplitude and $\phi_0(E)$ is an offset phase [22]. As shown in Fig. 4(a), the variation of asymmetry $A(E, \phi)$ with CEP is periodic, where all extrema are separated by $\Delta\phi = \pi$. For $y = 0$ we find, as expected, $|A(E, \phi)| = |A(E, \phi + \pi)|$.

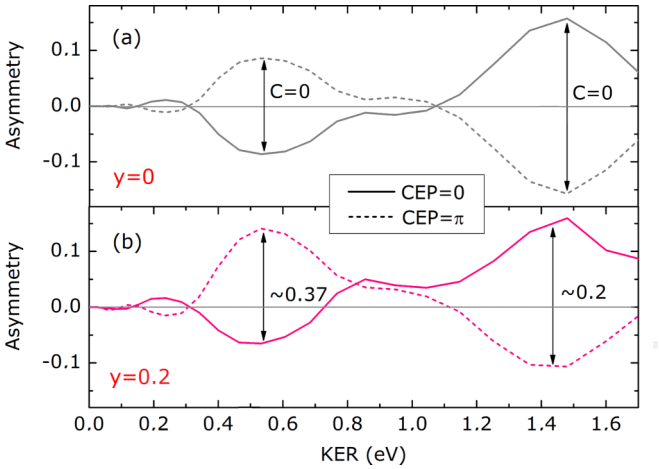

FIG. 3. Variation of the dissociation asymmetry A as a function of KER for (a) $y = 0$ and (b) $y = 0.2$ and for two different CEP values. The asymmetry contrast C is indicated for two KER points.

The periodicity in CEP variation is still largely valid for inhomogeneous fields with parameters as high as $y = 0.2$ [Fig. 4(b)]. Except for the low-KER region, there are no clearly apparent changes in the asymmetry maps. Differences become more evident in integrated asymmetries $[\int A(E, \phi)dE]$, as shown in Figs. 3(c)–3(f). Here we choose

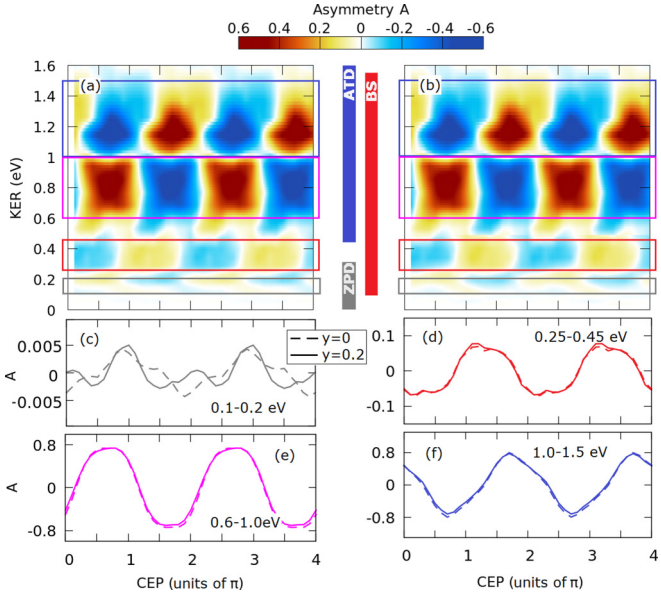

FIG. 4. Asymmetry maps $A(E, \phi)$ for dissociation of H_2^+ for (a) $y = 0$ and (b) $y = 0.2$. (c)–(f) The CEP variation of integrated asymmetry for different KER ranges as indicated in (a) and (b) for $y = 0$ (dashed lines) and $y = 0.2$ (solid lines).

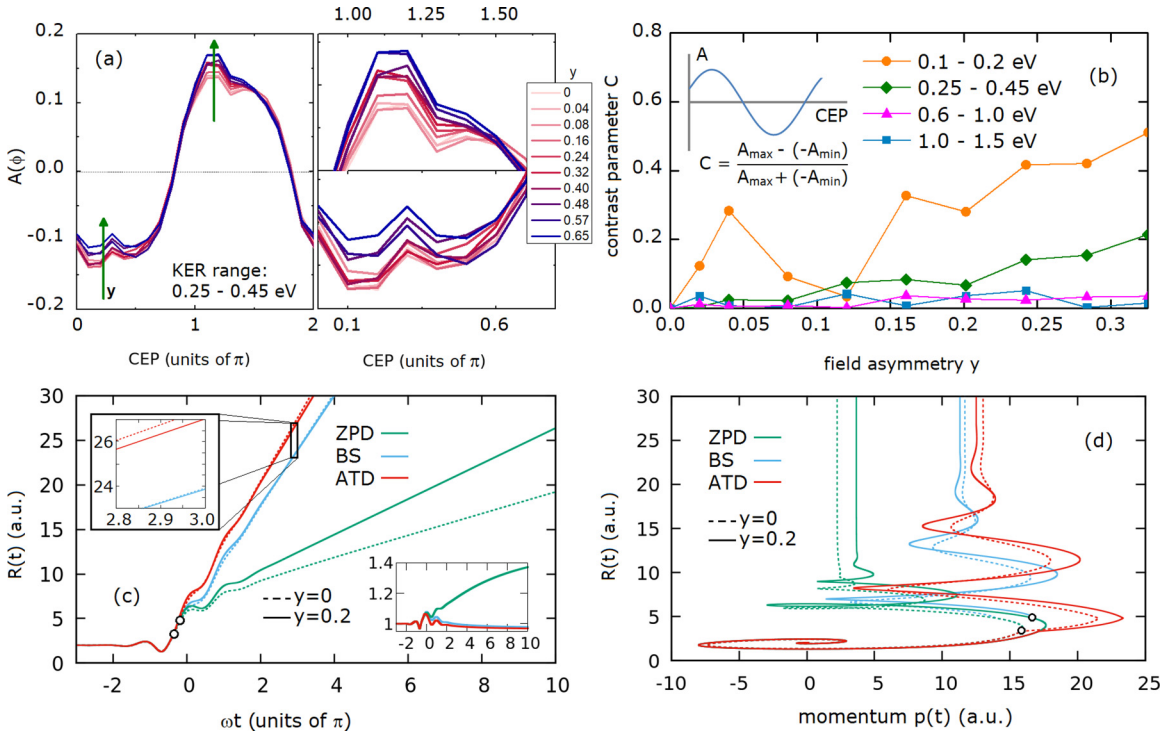

FIG. 5. (a) The CEP variation of the integrated asymmetry for different field asymmetries y. The arrows indicate the systematic up-shift of A (see the text). (b) Variation of contrast C between the maximum and minimum A for different KER ranges and as a function of y. (c) and (d) Results of the semiclassical dynamics of different dissociation channels for the case of $y = 0$ and $y = 0.2$. (c) Time variation of the dynamical distance $R(t)$ for $\phi = 0$. The top left inset shows a closeup of the time variation of $R(t)$ for the BS and ATD channels. The bottom right inset shows the ratio between $R(t)$ for $y = 0$ and $y = 0.2$. (d) Trajectory of dissociation of H_2^+. The black circles indicate moments of photon transitions.

KER ranges depicted in Figs. 4(a) and 4(b) with the intention of avoiding both overlap between dissociation channels and cancellation of asymmetry. Again the extrema are separated by π; however, we find that $|A(E,\phi)| \neq |A(E,\phi+\pi)|$. The impact of y on the breaking of the π periodicity of $|A|$ is stronger for the low-KER range (0.1–0.2 eV). Here $A_{\max}$ increases by 25% and $A_{\min}$ decreases by 30% from $y = 0$ to $y = 0.2$. Furthermore, for varying y values, the CEP variation of $A(\phi)$ is systematically upshifted due to directional control of y, as shown exemplarily in Fig. 5(a) for the (0.25–0.5)-eV range. This means that, with nonzero y, electrons are more likely localized on the left nucleus, i.e., higher fields. If we calculate the contrast between the maximum and the minimum of the asymmetry variation as $C = [A_{\max} - (-A_{\min})]/[A_{\max} + (-A_{\min})]$, we find that the contrast almost linearly increases within the studied y range as shown in Fig. 5(b). This observation is consistent with our wave-packet dynamics analysis (cf. Fig. 2) for low-energy regions, suggesting that these regions are largely responsible for higher contrast. Starting from $y = 0$, the contrast parameter increases from $C = 0$ up to $C = 0.2$ when $y = 0.32$. We evaluate the contrast for different KER ranges and different y values in Fig. 5(b). A strong control of C by y in the low-KER regions is observed, which we attribute to ZPD. The control is weak in the higher-KER regions, where BS and ATD are dominant. The impact of y on the contrast for different KER regions suggests that the length scale (i.e., stretching of the molecule) for photon transitions associated with a certain dissociation channel is a crucial factor, as illustrated in Fig. 1(c). The impact of y is enhanced for larger distances relative to the molecular center [see Fig. 1(b)] and each dissociation channel acquires a different degree of stretching (∼10, ∼5, and ∼3 a.u. for ZPD, BS, and ATD, respectively) before a transition to the repulsive state. The different behaviors seen in Figs. 4(a)–4(f) suggest that the spatial inhomogeneity of the near field provides an additional mechanism for controlling chemical reactions.

To qualitatively address the physical mechanism behind the channel dependence of the impact of the field asymmetry, we devise a semiclassical two-state model based on the dynamics of a particle in an inhomogeneous field $\mu_p \ddot{R} = -\partial_R[D_{g,u}(R) + V(R,t;y)]$. Here μ_p is the reduced proton mass, $D_g(R)$ and $D_u(R)$ are the potentials of $1s\sigma_g$ and $2p\sigma_u$ states presented in Fig. 1(c), respectively, and $V(R,t;y)$ is the interaction potential approximated from Eq. (2). The system is initially assumed to be in the equilibrium distance of 2 a.u. with zero momentum. The semiclassical dynamics are simulated for different dissociation channels by executing the nonclassical interstate transitions (for BS and ATD) at the moment the resonance condition (i.e., R distance where the potential energy curves differ by a multiple of $\hbar\omega$) is met. One can see that a certain amount of stretching is necessary for the BS, ATD, and ZPD channels to be activated [as can be understood from Fig. 1(c)], which can then be coupled with the length scale of the field asymmetry. Considering the time variation of R, in Fig. 5(c), we see that BS and ATD channels

are activated at the rising edge of the field at relatively short distances, where the influence of y is relatively small. On the other hand, ZPD strives for longer intermolecular distances, which coalesce with increasing impact of y. As a result, both BS and ATD are less affected by the field asymmetry than ZPD. Figure 5(d) shows semiclassical trajectories in an inhomogeneous field represented in the phase space. In all cases, the particle first oscillates under the field and later dissociates, attaining a constant momentum. The ZPD occurs very slowly relative to the other states but gains extra momentum with field asymmetry. Trajectories of both BS and ATD are visibly less affected by y. Our semiclassical analysis clearly shows that the length scale of the dissociation channel is critical for the dissociation control of y.

IV. CONCLUSION

We have studied the control of dissociation of the H_2^+ molecular ion by spatially inhomogeneous fields, i.e., field asymmetry, with TDSE simulations. The field inhomogeneity results in a breaking of the inversion symmetry of the CEP-dependent dissociation direction asymmetry. We investigated the ZPD, BS, and ATD channels in more detail and found that the field asymmetry length scale, given by the y parameter, and the length scale of the various dissociation reactions determine how much a certain reaction channel is affected and controlled by the inhomogeneity. Our results pave the way towards using spatially inhomogeneous near fields as a control mechanism for the manipulation of electron and nuclear dynamics in molecules driven by intense laser fields.

ACKNOWLEDGMENTS

The authors are thankful to A. Chacón, P. Rupp, and B. Bergues for valuable discussions. Calculations were performed at the Simulations and Research Laboratory, Physics Department of MU, supported by Grant No. FEN-A-100616-0275 by BAPKO. M.F.C., P.R., J.S., and M.F.K. acknowledge support by the DFG through the center of excellence "Munich Centre for Advanced Photonics." M.F.K. is grateful for support from the EU via the ERC grant ATTOCO. M.L. acknowledges the Spanish Ministry MINECO (National Plan 15 Grants FISICATEAMO No. FIS2016-79508-P, SEVERO OCHOA No. SEV-2015-0522, FPI), European Social Fund, Fundació Cellex, Generalitat de Catalunya (AGAUR Grant No. 2017 SGR 1341 and CERCA/Program), ERC AdG OSYRIS, EU FETPRO QUIC, and the National Science Centre, Poland-Symfonia Grant No. 2016/20/W/ST4/00314. This work was supported by the Project "Advanced research using high intensity laser produced photons and particles" (No. CZ.02.1.01/0.0/0.0/16_019/0000789) from European Regional Development Fund (ADONIS).

[1] X. M. Tong and C. D. Lin, J. Phys. B **40**, 641 (2007).
[2] P. H. Bucksbaum, A. Zavriyev, H. G. Muller, and D. W. Schumacher, Phys. Rev. Lett. **64**, 1883 (1990).
[3] A. Zavriyev, P. H. Bucksbaum, J. Squier, and F. Saline, Phys. Rev. Lett. **70**, 1077 (1993).
[4] L. J. Frasinski, J. H. Posthumus, J. Plumridge, K. Codling, P. F. Taday, and A. J. Langley, Phys. Rev. Lett. **83**, 3625 (1999).
[5] H. Abou-Rachid, T. Tung Nguyen-Dang, and O. Atabek, J. Chem. Phys **110**, 4737 (1999).
[6] K. Sändig, H. Figger, and T. W. Hänsch, Phys. Rev. Lett. **85**, 4876 (2000).
[7] X. M. Tong, Z. X. Zhao, and C. D. Lin, Phys. Rev. A **68**, 043412 (2003).
[8] J. H. Posthumus, Rep. Prog. Phys. **67**, 623 (2004).
[9] F. He, A. Becker, and U. Thumm, Phys. Rev. Lett. **101**, 213002 (2008).
[10] B. Fischer, M. Kremer, T. Pfeifer, B. Feuerstein, V. Sharma, U. Thumm, C. D. Schröter, R. Moshammer, and J. Ullrich, Phys. Rev. Lett. **105**, 223001 (2010).
[11] F. Anis and B. D. Esry, Phys. Rev. Lett. **109**, 133001 (2012).
[12] J. McKenna, F. Anis, A. M. Sayler, B. Gaire, N. G. Johnson, E. Parke, K. D. Carnes, B. D. Esry, and I. Ben-Itzhak, Phys. Rev. A **85**, 023405 (2012).
[13] F. Kelkensberg, G. Sansone, M. Y. Ivanov, and M. Vraking, Phys. Chem. Chem. Phys. **13**, 8647 (2011).
[14] K. F. Lee, F. Légaré, D. M. Villeneuve, and P. B. Corkum, J. Phys. B **39**, 4081 (2006).
[15] Y.-J. Jin, X.-M. Tong, and N. Toshima, Phys. Rev. A **86**, 053418 (2012).
[16] X. Chu and S.-I. Chu, Phys. Rev. A **63**, 023411 (2001).
[17] A. D. Bandrauk, S. Chelkowski, and H. S. Nguyen, Int. J. Quantum Chem. **100**, 834 (2004).
[18] V. Roudnev, B. D. Esry, and I. Ben-Itzhak, Phys. Rev. Lett. **93**, 163601 (2004).
[19] M. F. Kling, C. Siedschlag, A. J. Verhoef, J. I. Khan, M. Schultze, T. Uphues, Y. Ni, M. Uiberacker, M. Drescher, F. Krausz, and M. J. J. Vrakking, Science **312**, 246 (2006).
[20] X. M. Tong and C. D. Lin, Phys. Rev. Lett. **98**, 123002 (2007).
[21] S. Gräfe and M. Y. Ivanov, Phys. Rev. Lett. **99**, 163603 (2007).
[22] M. F. Kling, C. Siedschlag, I. Znakovskaya, A. J. Verhoef, S. Zherebtsov, F. Krausz, M. Lezius, and M. J. J. Vrakking, Mol. Phys. **106**, 455 (2008).
[23] D. Geppert, P. con den Hoff, and R. de Vivie-Riedle, J. Phys. B **41**, 074006 (2008).
[24] J. J. Hua and B. D. Esry, J. Phys. B **42**, 085601 (2009).
[25] M. Kremer, B. Fischer, B. Feuerstein, V. L. B. de Jesus, V. Sharma, C. Hofrichter, A. Rudenko, U. Thumm, C. D. Schröter, R. Moshammer, and J. Ullrich, Phys. Rev. Lett. **103**, 213003 (2009).
[26] P. von den Hoff, I. Znakovskaya, M. F. Kling, and R. de Vivie-Riedle, Chem. Phys. **366**, 139 (2009).
[27] I. Znakovskaya, P. von den Hoff, G. Marcus, S. Zherebtsov, B. Bergues, X. Gu, Y. Deng, M. J. J. Vrakking, R. Kienberger, F. Krausz, R. de Vivie-Riedle, and M. F. Kling, Phys. Rev. Lett. **108**, 063002 (2012).
[28] F. He, Phys. Rev. A **86**, 063415 (2012).
[29] M. F. Kling, P. von den Hoff, I. Znakovskaya, and R. de Vivie-Riedle, Phys. Chem. Chem. Phys. **15**, 9448 (2013).
[30] T. Rathje, A. M. Sayler, S. Zeng, P. Wustelt, H. Figger, B. D. Esry, and G. G. Paulus, Phys. Rev. Lett. **111**, 093002 (2013).

[31] N. G. Kling, K. J. Betsch, M. Zohrabi, S. Zeng, F. Anis, U. Ablikim, B. Jochim, Z. Wang, M. Kübel, M. F. Kling, K. D. Carnes, B. D. Esry, and I. Ben-Itzhak, Phys. Rev. Lett. **111**, 163004 (2013).

[32] H. Xu, J. P. Maclean, W. C. Laban, D. Kielpinski, R. T. Sang, and I. V. Litvinyuk, New J. Phys. **15**, 023034 (2013).

[33] H. Xu, T.-Y. Xu, F. He, D. Kielpinski, R. T. Sang, and I. V. Litvinyuk, Phys. Rev. A **89**, 041403(R) (2014).

[34] H. Li, A. S. Alnaser, X. M. Tong, K. J. Betsch, M. Kübel, T. Pischke, B. Förg, J. Schötz, F. Süßmann, S. Zherebtsov, B. Bergues, A. Kessel, S. A. Trushin, A. M. Azzeer, and M. F. Kling, J. Phys. B **47**, 124020 (2014).

[35] F. Krausz and M. Ivanov, Rev. Mod. Phys. **81**, 163 (2009).

[36] P. Hommelhoff and M. F. Kling, *Attosecond Nanophysics* (Wiley-VCH, Weinheim, 2015).

[37] M. F. Ciappina *et al.*, Rep. Prog. Phys. **80**, 054401 (2017).

[38] P. Hommelhoff, Y. Sortais, A. Aghajani-Talesh, and M. A. Kasevich, Phys. Rev. Lett. **96**, 077401 (2006).

[39] C. Ropers, D. R. Solli, C. P. Schulz, C. Lienau, and T. Elsaesser, Phys. Rev. Lett. **98**, 043907 (2007).

[40] R. Bormann, M. Gulde, A. Weismann, S. V. Yalunin, and C. Ropers, Phys. Rev. Lett. **105**, 147601 (2010).

[41] M. Schenk, M. Krüger, and P. Hommelhoff, Phys. Rev. Lett. **105**, 257601 (2010).

[42] H. Yanagisawa, M. Hengsberger, D. Leuenberger, M. Klöckner, C. Hafner, T. Greber, and J. Osterwalder, Phys. Rev. Lett. **107**, 087601 (2011).

[43] D. J. Park, B. Piglosiewicz, S. Schmidt, H. Kollmann, M. Mascheck, and C. Lienau, Phys. Rev. Lett. **109**, 244803 (2012).

[44] P. Dombi, A. Hörl, P. Rácz, I. Márton, A. Trügler, J. R. Krenn, and U. Hohenester, Nano Lett. **13**, 674 (2013).

[45] L. Wimmer, G. Herink, D. R. Solli, S. V. Yalunin, K. E. Echterkamp, and C. Ropers, Nat. Phys. **10**, 432 (2014).

[46] B. Piglosiewicz, S. Schmidt, D. J. Park, J. Vogelsang, P. Groß, C. Manzoni, P. Farinello, G. Cerullo, and C. Lienau, Nat. Photon. **8**, 37 (2014).

[47] J. Vogelsang, J. Robin, B. J. Nagy, P. Dombi, D. Rosenkranz, M. Schiek, P. Groß, and C. Lienau, Nano Lett. **15**, 4685 (2015).

[48] H. Yanagisawa, S. Schnepp, C. Hafner, M. Hengsberger, D. Kim, M. F. Kling, A. Landsman, L. Gallmann, and J. Osterwalder, Sci. Rep. **6**, 35877 (2016).

[49] K. E. Echternkamp, G. Herink, S. V. Yalunin, K. Rademann, S. Schäfer, and C. Ropers, Appl. Phys. B **122**, 80 (2016).

[50] S. Li and R. R. Jones, Nat. Commun. **7**, 13405 (2016).

[51] J. Schötz, S. Mitra, H. Fuest, M. Neuhaus, W. A. Okell, M. Förster, T. Paschen, M. F. Ciappina, H. Yanagisawa, P. Wnuk, P. Hommelhoff, and M. F. Kling, Phys. Rev. A **97**, 013413 (2018).

[52] E. Peralta, K. Soong, R. England, E. Colby, Z. Wu, B. Montazeri, C. McGuinness, J. McNeur, K. Leedle, D. Walz *et al.*, Nature (London) **503**, 91 (2013).

[53] J. Breuer and P. Hommelhoff, Phys. Rev. Lett. **111**, 134803 (2013).

[54] S. Zherebtsov, T. Fennel, J. Plenge, E. Antonsson, I. Znakovskaya, A. Wirth, O. Herrwerth, F. Süßmann, C. Peltz, I. Ahmad, S. A. Trushin, V. Pervak, S. Karsch, M. J. J. Vrakking, B. Langer, C. Graf, M. I. Stockman, F. Krausz, E. Rühl, and M. F. Kling, Nat. Phys. **7**, 656 (2011).

[55] M. Krüger, M. Schenk, and P. Hommelhoff, Nature (London) **475**, 78 (2011).

[56] G. Wachter, C. Lemell, J. Burgdörfer, M. Schenk, M. Krüger, and P. Hommelhoff, Phys. Rev. B **86**, 035402 (2012).

[57] S. Zherebtsov, F. Süßmann, C. Peltz, J. Plenge, K. J. Betsch, I. Znakovskaya, A. S. Alnaser, N. G. Johnson, M. Kübel, A. Horn, V. Mondes, C. Graf, S. A. Trushin, A. Azzeer, M. J. J. Vrakking, G. G. Paulus, F. Krausz, E. Rühl, T. Fennel, and M. F. Kling, New J. Phys. **14**, 075010 (2012).

[58] G. Herink, D. Solli, M. Gulde, and C. Ropers, Nature (London) **483**, 190 (2012).

[59] F. Süßmann, L. Seiffert, S. Zherebtsov, V. Mondes, J. Stierle, M. Arbeiter, J. Plenge, P. Rupp, C. Peltz, A. Kessel, S. A. Trushin, B. Ahn, D. Kim, C. Graf, E. Rühl, M. F. Kling, and T. Fennel, Nat. Commun. **6**, 7944 (2015).

[60] L. Seiffert, P. Henning, P. Rupp, S. Zherebtsov, P. Hommelhoff, M. F. Kling, and T. Fennel, J. Mod. Opt. **64**, 1096 (2017).

[61] P. Rupp, L. Seiffert, Q. Liu, F. Süßmann, B. Ahn, B. Förg, C. G. Schäfer, M. Gallei, V. Mondes, A. Kessel, S. Trushin, C. Graf, E. Rühl, J. Lee, M. S. Kim, D. E. Kim, T. Fennel, M. F. Kling, and S. Zherebtsov, J. Mod. Opt. **64**, 995 (2017).

[62] S. Han, H. Kim, Y. W. Kim, Y.-J. Kim, S. Kim, I.-Y. Park, and S.-W. Kim, Nat. Commun. **7**, 13105 (2016).

[63] M. Sivis, M. Taucer, G. Vampa, K. Johnston, A. Staudte, A. Y. Naumov, D. M. Villeneuve, C. Ropers, and P. B. Corkum, Science **357**, 303 (2017).

[64] B. Förg, J. Schötz, F. Süßmann, M. Förster, M. Krüger, B. Ahn, W. A. Okell, K. Wintersperger, S. Zherebtsov, A. Guggenmos, V. Pervak, A. Kessel, S. A. Trushin, A. M. Azzeer, M. I. Stockman, D. Kim, F. Krausz, P. Hommelhoff, and M. F. Kling, Nat. Commun. **7**, 11717 (2016).

[65] J. Schötz, B. Förg, M. Förster, W. A. Okell, M. I. Stockman, F. Krausz, P. Hommelhoff, and M. F. Kling, IEEE J. Sel. Top. Quantum Electron. **23**, 77 (2017).

[66] S. Choi, M. F. Ciappina, J. A. Pérez-Hernández, A. S. Landsman, Y.-J. Kim, S. C. Kim, and D. E. Kim, Phys. Rev. A **93**, 021405(R) (2016).

[67] E. Kazuma, J. Jung, H. Ueba, M. Trenary, and Y. Kim, Science **360**, 521 (2018).

[68] I. Yavuz, M. F. Ciappina, A. Chacón, Z. Altun, M. F. Kling, and M. Lewenstein, Phys. Rev. A **93**, 033404 (2016).

[69] B. Feuerstein and U. Thumm, Phys. Rev. A **67**, 043405 (2003).

[70] L. Novotny and B. Hecht, *Principles of Nano-Optics* (Cambridge University Press, Cambridge, 2012).

[71] S. Thomas, G. Wachter, C. Lemell, J. Burgdörfer, and P. Hommelhoff, New J. Phys. **17**, 063010 (2015).

[72] M. Bionta, S. Weber, I. Blum, J. Mauchain, B. Chatel, and B. Chalopin, New J. Phys. **18**, 103010 (2016).

[73] M. Yamaguchi and K. Nobusada, Phys. Rev. A **93**, 023416 (2016).

[74] A. Giusti-Suzor, X. He, O. Atabek, and F. H. Mies, Phys. Rev. Lett. **64**, 515 (1990).

[75] B. Feuerstein and U. Thumm, J. Phys. B **36**, 707 (2003).